Journal of King Saud University – Engineering Sciences (2016) **28**, 110–118

King Saud University

Journal of King Saud University – Engineering Sciences

www.ksu.edu.sa
www.sciencedirect.com

ORIGINAL ARTICLE

Evaluation of palm kernel fibers (PKFs) for production of asbestos-free automotive brake pads

K.K. Ikpambese *, D.T. Gundu, L.T. Tuleun

Department of Mechanical Engineering, University of Agriculture, p.m.b. 2373, Makurdi, Nigeria

Received 12 August 2013; accepted 6 February 2014
Available online 18 February 2014

KEYWORDS

Brake pads;
Friction coefficient;
Palm kernel fibres;
Wear rate;
Asbestos

Abstract In this study, asbestos-free automotive brake pads produced from palm kernel fibers with epoxy-resin binder was evaluated. Resins varied in formulations and properties such as friction coefficient, wear rate, hardness test, porosity, noise level, temperature, specific gravity, stopping time, moisture effects, surface roughness, oil and water absorptions rates, and microstructure examination were investigated. Other basic engineering properties of mechanical overload, thermal deformation fading behaviour shear strength, cracking resistance, over-heat recovery, and effect on rotor disc, caliper pressure, pad grip effect and pad dusting effect were also investigated. The results obtained indicated that the wear rate, coefficient of friction, noise level, temperature, and stopping time of the produced brake pads increased as the speed increases. The results also show that porosity, hardness, moisture content, specific gravity, surface roughness, and oil and water absorption rates remained constant with increase in speed. The result of microstructure examination revealed that worm surfaces were characterized by abrasion wear where the asperities were ploughed thereby exposing the white region of palm kernel fibers, thus increasing the smoothness of the friction materials. Sample S_6 with composition of 40% epoxy-resin, 10% palm wastes, 6% Al_2O_3, 29% graphite, and 15% calcium carbonate gave better properties. The result indicated that palm kernel fibers can be effectively used as a replacement for asbestos in brake pad production.

1. Introduction

Brake pads are used in the braking systems of automobiles and other vehicles and machines to control the speed by converting kinetic energy of the vehicles to heat which is dissipated to the atmosphere. Brake pads are steel backing plate with friction material bound to the surface facing the disc (Idris et al., 2015). The demands on the brake pads are such that they must maintain a sufficiently high friction coefficient with the disc; not decompose or break down in such a way that the friction coefficient with the brake disc is not compromised at high temperatures; exhibit a stable and constant friction coefficient with the brake disc (Efendy et al., 2010).

According to Idris et al. (2015) brake pads generally consist of asbestos embedded in the polymeric matrix along with several other ingredients. That the use of asbestos is being avoided

* Corresponding author. Tel.: +234 7036850364.
E-mail address: kikpambese@yahoo.com (K.K. Ikpambese).
Peer review under responsibility of King Saud University.

ELSEVIER Production and hosting by Elsevier

1018-3639 © 2014 Production and hosting by Elsevier B.V. on behalf of King Saud University.
http://dx.doi.org/10.1016/j.jksues.2014.02.001

due to its carcinogenic and harmful nature new asbestos free materials and brake pads have been developed.

Agricultural residues or wastes are now emerging as new and inexpensive materials in the brake pads' development with commercial viability and environmental acceptability. Idris et al. (2015) produced an eco-friendly asbestos free brake pads using banana peels and the findings concluded that banana peels can be effectively used as to replace. Namessan et al. (2012) developed brake pads from kenaf (*Hibiscus canabinus*) fibres, using different treatments. Koya and Fono (2010) developed automotive brake pad using palm kernel shell following the standard procedures employed by commercial manufacturers and the result obtained showed that the properties of palm kernel shell based brake pad wholly satisfied the recommendation of the Standard Organization of Nigeria (SON).

Also, development of asbestos-free brake pad using bagasse was reported by Aigbodion et al. (2010). Ibhadode and Dagwa (2008), developed asbestos-free friction lining materials from palm kernel shell and when compared with a premium asbestos-based commercial brake pad they were found to perform satisfactorily. Palm slag was also employed by Ruzaidi et al. (2011) for the production of brake pads; results indicated that palm slag can be used effectively as an alternative to in brake pad composites.

This research paper aims to evaluate properties of asbestos – free automotive brake pads produced from palm kernel fibres and to compare it with the commercial brake pad.

2. Materials and methods

2.1. Preparation of the raw materials

Palm kernel fibers (PKFs) were collected and suspended in a solution of caustic soda (sodium hydroxide) for twenty four hours to remove the remnant of red oil left after extraction. The fibers as shown in Fig. 1 were then washed with water to remove the caustic soda and sun dried for one week. The dried PKFs was grounded into powder form using a Hammer mill and was thereafter sieved using sieve size $\leqslant$100 μm aperture.

2.2. Characterization of palm kernel fibre

The elemental composition of the PKFs was determined using X-Ray Fluorescence (XRF) machine. The powder sample of PKFs was initially pulverized using Agate/pestle. Pulverization of the sample was necessary to ensure homogenization of the sample. A measured mass of 5 g of pulverized PKFs was formed into pellets in a pelletizer with hydraulic press. Pelletization was done to aid the removal of voids between the particles of the sample and to ensure a better interaction of the sample with the primary X-ray from the x-ray tube which excites the atoms in the sample giving x-rays flouresence/characteristics. The pellets were sealed into the chamber of the XRF (Amptek Inc) and allowed to run for 1000 s at a voltage of 25 kV, and a current of 50 μA and excited by the primary x-ray source from the x-ray tube. The x-ray detector inclined at 90° to the primary x-ray source picks up characteristic x-rays which were amplified and the signal from the amplifier was processed by multichannel analyzer and relayed to the computer where the data was acquired by the appropriate software. The acquired data was then analyzed using Axil customized software for the determination of the elemental composition of the materials.

Figure 1 Fibres of palm kernel.

Figure 2 The produced brake pads.

2.3. Development of the brake pad

The production of brake pad consists of a series of unit operations including mixing, cold and hot pressing, cooling, post-curing and finishing (Koya and Fono, 2010).

The sieve size of 100 μm of PKFs was added in varying percentages to aluminium oxide, calcium carbonate and epoxy resin (Table 1) based on 176 g weight of commercial brake pad. The combinations were separately dry-mixed using a blender in order to achieve a homogeneous state ready for molding.

The mixtures for each of the formulations were separately transferred into a designed mould placed on the backing plate obtained by removing the friction materials on the used commercial brake pad. The mould containing the friction materials

Table 1 Additives used for brake pads production from palm kernel fibre (PKFs).

Brake additives	Samples in percentage weight (% wt)					
	S_1	S_2	S_3	S_4	S_5	S_6
Epoxy resin	15	19	23	25	30	40
Palm kernel fibres (PKFs)	35	6	27	30	40	10
Aluminium oxide	5	0	10	5	5	6
Graphite	5	5	10	5	5	29
Calcium carbonate	40	70	30	35	20	15

was pressed at 100 KN force for 2 minutes at room temperature. The produced brake pads were cured at 250 °C for 90 min after removal from the hydraulic press.

The produced samples were finished by polishing them using polisher-grinder with various grinding paper of various sizes to obtain the final products. The produced samples are presented on Fig. 2.

2.4. Evaluation of the developed brake pads

2.4.1. Test procedure using Inertia dynamometer

The Inertia dynamotor with the following specifications presented in Table 2 located at Anambra State Motor Manufacturing Company (ANAMMCO) Nigeria was used for the evaluation of the developed brake pads.

Each pair of developed brake pads separately mounted on the brake assembly unit of the inertia dynamometer shown in Fig. 3, is driven by electric motor through shaft-coupling. The rotating speed of the motor was initially set at 5.56 m/s by using variable speed drive with tachometer and brake was applied after attaining the set speed with the measured values of wear rate, coefficient of friction through a computer connected to it. This procedure was repeated for speeds 8.33, 11.11, 16.67, 22.22 and 27.78 m/s to obtain the corresponding values of wear rate and coefficient of friction.

Numerous Sensors attached to the brake pad assembly unit were able to measure other parameters at speeds 5.5, 33, 11.11, 6.67, 22.22 and 27.78 m/s through a computer connected to the machine. The parameters measured were hardness, porosity, braking pressure, noise level, thermal temperature, specific gravity, stopping time, moisture effects, and oil and water absorptions. Other engineering properties evaluated at a constant speed of 27.78 m/s (100 km/h) were mechanical overload, thermal deformation fading behaviour, shear strength, cracking resistance over-heat recovery, effect on rotor disc, caliper pressure, pad grip effect and pad dusting effect. This procedure was repeated for the commercial brake pad (Auto-boss) obtained from the market for comparison.

2.5. Micro-structure analysis

The micro structural analysis for unworn and worm surfaces of the produced brake pad samples were viewed on a Digital Metallurgical Microscope to describe the wear pattern and the distribution of various additives in the friction materials. This was achieved by clamping the specimen on the mechanical stage of the microscope, adjusting the lens of microscope using adjustment knob until clear image was observed at magnification of 4 and was later captured on a computer connected to it with the aid of software.

3. Results and discussion

3.1. Elemental composition of palm kernel fibre (PKFs)

Table 3 presents the elemental compositions of PKFs. The result revealed that PKFs mainly contains semi-metals and non-metals. These elements are equally found in asbestos which

Table 2 Inertia dynamometer machine specification.

S/N	Specifications	Drive
1	Max drive power	375 kW (540 HP)
2	Max drive torque	2527 Nm
3	Max drive speed	2500 rpm (400 km/h)
4	Max brake torque	25,000 Nm
5	Pressure brake	6000 N*2
6	Flywheel inertia	Max/min (1900/400 kg m^2)
7	Diameter of test wheel	Ø 700, 1120 mm
8	Acceleration time	1 min 30 s

Table 3 Elemental composition of palm kernel fibres (PKFs).

Elements	Concentration value	Concentration error	Unit
K	860	± 57	Ppm
Ca	1136	± 58	Ppm
Ba	101	± 25	Ppm
Cr	191	± 21	Ppm
Mn	116	± 11	Ppm
Fe	1254	± 34	Ppm
Ni	3	± 0	Ppm
Cu	18	± 1	Ppm
Zn	127	± 6	Ppm
Se	54	± 7	Ppm
Sr	141	± 20	Ppm
Br	30	± 4	Ppm
Pb	9	± 2	Ppm

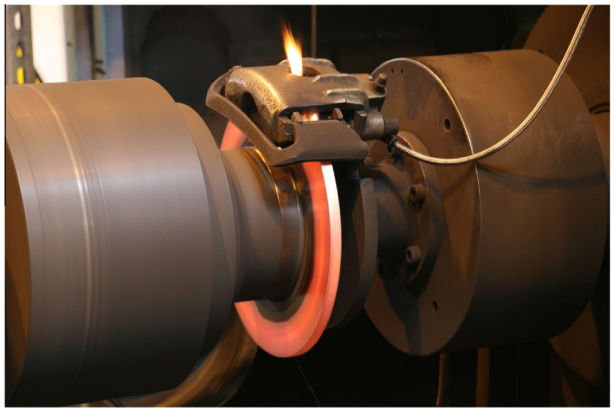

Figure 3 Brake assembly unit of the Inertia dynamometer.

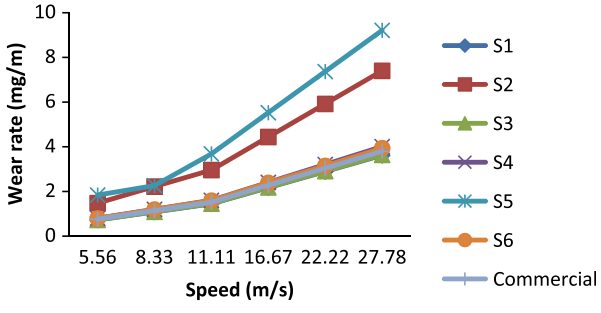

Figure 4 Variation of wear rate with speed.

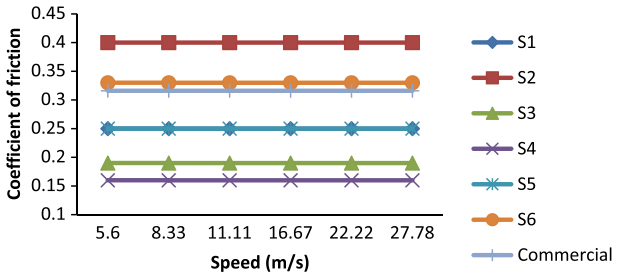

Figure 5 Variation of coefficient of friction with speed.

suggested that PKFs can be used as fibres in the production of brake pads. These reports confirmed the earlier result obtained by Koya and Fono (2010).

3.2. Wear rate

Fig. 4 shows the variation of wear rate with speed for brake pads produced from PKFs along with the commercial brake pad. It was observed that the wear rates increased as speed increases for all the samples produced as well as the commercial brake pad. Wear rate data were different for different formulations due to different additives and their weight percentages used in their compositions. The increase in speed leads to increase in contact pressure between the rotor and brake pads, thus increased wear rate. This trend was reported by Ibhadode and Dagwa (2008). The wear rate for brake pads was produced at 27.7 m/s (100 km/h) as shown on Fig. 4 and varied from 3.62–9.21 mg/m. Samples S_1 (3.62), and S_3, (3.64 mg/m), exhibited less wear rate compared to the commercial brake pad (3.8 mg/m). These wear rates were better compared with the values of 4.20 and 4.40 mg/m reported by Aigbodion et al. (2010). The lowest values of wear rate obtained from the produced brake pads could be attributed to the type of binder used and it is obvious that the epoxy resin used for the formulation of the pads provides a better bonding of the friction materials that resist wear rates.

3.3. Coefficient of friction

Change in brake's coefficient of friction as a function of speed is a very important issue because drivers expect the same level of friction force at various conditions (Jang et al., 2004), and the coefficient of friction material often varies as the speed changes. Fig. 5 showed that coefficient of friction obtained from brake pads produced along with commercial brake pads maintained constant coefficient of friction as the speed changes from 5.56 to 27.78 m/s. The values of coefficient of friction obtained varied from 0.16–0.4. The values of coefficient of friction for samples S_1 (0.4), and S_2 (0.33) agreed with the values of 0.3–0.4 reported by El-Tayeb and Liew (2009), and was better compared to the value of 0.316 obtained from commercial pad.

The stable coefficient of friction observed may be due to non-inclusion of steel fibers. El-Tayeb and Liew (2009) reported that steel fibers play a major role in increasing the coefficient of friction and continuous increase of coefficient of friction is often associated with the adhesion of metal chips in the brake pad to the friction surface of the cast iron disc. This could also be attributed to non-formation of cold welding and rupture of asperities of the virgin brake pad surfaces as reported by Liew and Nirmal (2013). Hence, there were no detached asperities trapped between the sliding surfaces which could have caused an increase in the coefficient of friction. Another reason could be the inability of the formation rates of oxides due to high and flash temperature at the interface. El-Tayeb and Liew (2009) reported that certain oxides have lubricating characteristics and could assist the lubricant additives already included in the pad formulation to further reduce the friction.

3.4. Porosity

Fig. 6 presents the variation of porosity with speed for brake pads produced. It was observed that porosity remains constant as the speed was varied from 5.56 to 27.78 m/s. The porosity values of samples produced varied from 16% to 32% and the porosity values agreed with the values of 13–23% reported by Chand et al. (2004), 22.45% reported by Ibhadode and Dagwa (2008).

3.5. Hardness

Hardness of the produced brake pads as measured by the inertia dynamometer was the time (hours) it takes for the brake pads to return to its original form upon maximum stress. The variations of hardness with speed (5.65–27.78 m/s) as shown in Fig. 7 with the commercial brake pad remain constant as the speed was varied from 5.56 to 27.78 m/s. The hardness values of the produced samples varied from 5.6 to 21 h. were better compared to the values of 45.34–59.83 h reported by WanNik et al. (2012) and also agreed with the value of 9.83 h obtained by the commercial brake pads.

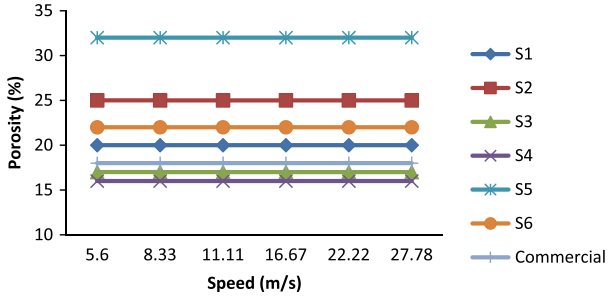

Figure 6 Variation of porosity with speed.

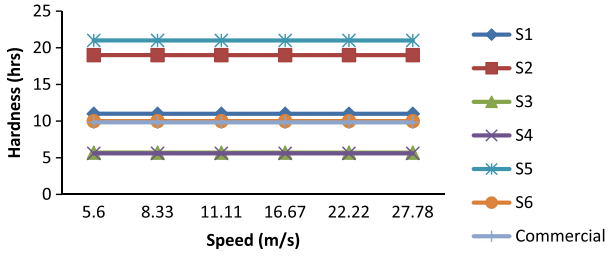

Figure 7 Variation of hardness with speed.

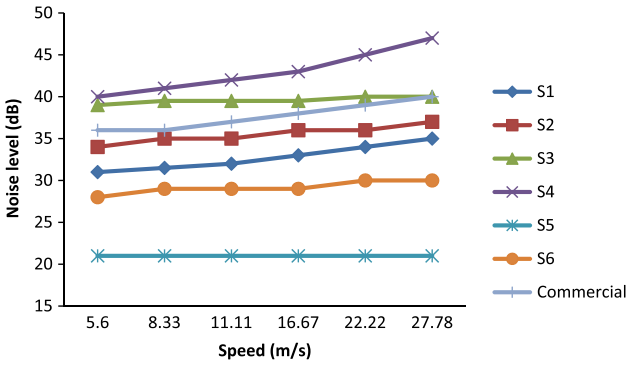

Figure 8 Variation of noise level with speed.

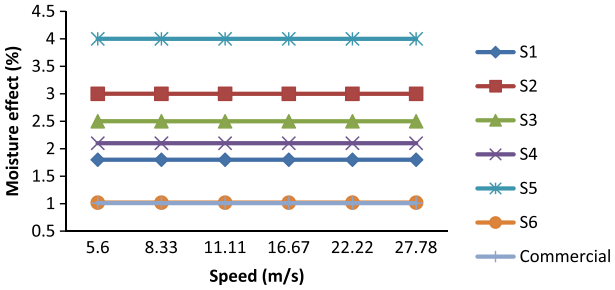

Figure 9 Variation of moisture effect with speed.

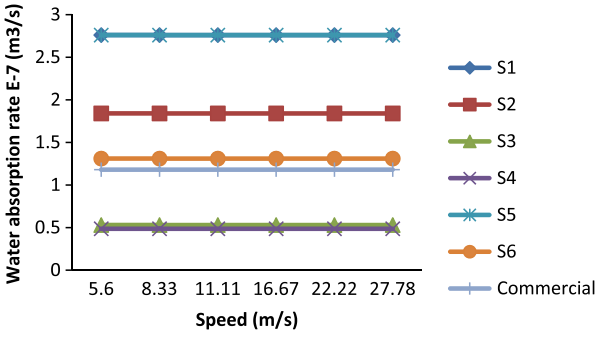

Figure 10 Variation of water absorption rate with speed.

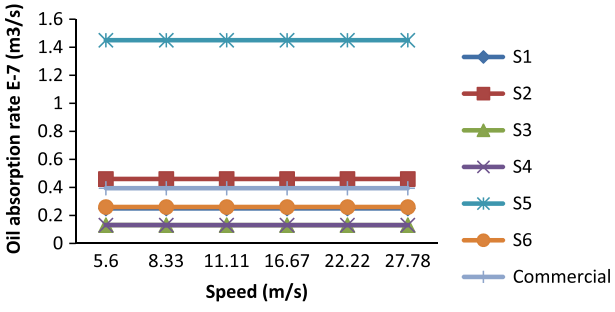

Figure 11 Variation of oil absorption rate with speed.

3.6. Noise level

Noise levels generated by the brake pads produced along with the commercial brake pad are presented in Fig. 8. It was observed that the noise level (excluding S_5) increased with increasing speed, and that the slope differed according to the formulations. This trend agrees with the results reported by Lindberg et al. (2013). The noise levels of samples produced varied from 21–47 dB. The noise levels obtained agreed with the value of 40 dB obtained by the commercial brake pad, standard values of 25–40 dB given by the inertia dynamometer, and the values of 25–29 dB reported by Lindberg et al. (2013). The lower noise levels exhibited by most of the produced brake pads could be due to non-inclusion of harder or aggressive particles in the formulation. Kim et al. (2011) reported that hard and abrasive particles can cause friction induced vibration which leads to noise than mild or no abrasives. Single-slot carved on the surfaces of the produced brake pads could be another possible reason for the lower noise level. This confirms the result reported by Oberst and Lai (2011) where the single-slotted pad performs better compared with the non slotted pad.

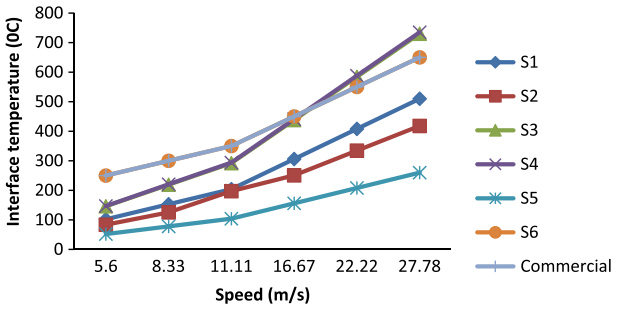

Figure 12 Variation of interface temperature with speed.

3.7. Moisture effect

The variation of moisture effects with speed is presented in Fig. 9 and shows that moisture effect remained constant as the speed was varied. The values of moisture effects of 1.02–2.5% of the produced brake pad samples S_2 (1.02%), compared well with the standard values of 0–2% given by the inertia dynamometer, while values of 1.02% and 1.04% from PKFs compared well with the value of 1.01% obtained by the commercial pad.

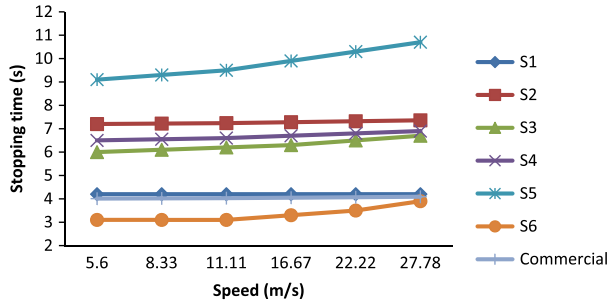

Figure 13 Variation of stopping time with speed.

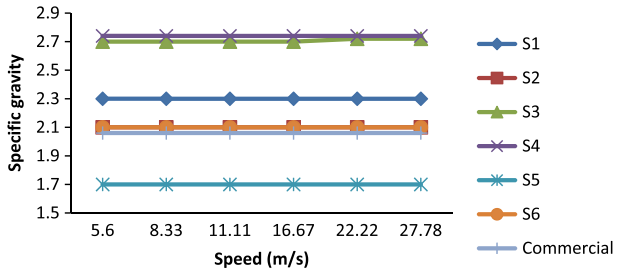

Figure 14 Variation of specific gravity with speed.

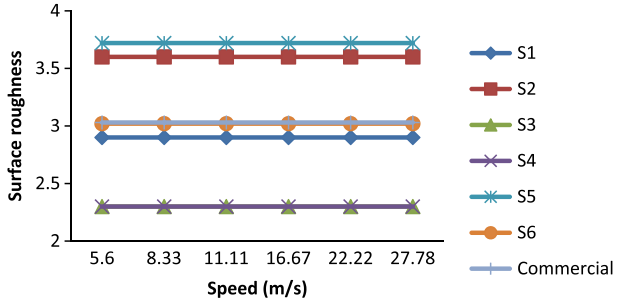

Figure 15 Variation of surface roughness rate with speed.

3.8. Water and oil absorption rates

The variation of water and oil absorption rates with speed for brake pads produced along with the commercial pad is presented in Figs. 10 and 11 respectively. The water and oil absorption rates for the produced samples including the commercial pad were constant as the speed varied. The water and oil absorption rates varied from 3.9×10^{-8}–1.31×10^{-7} m^3/s to 0.113×10^{-7}–1.45×10^{-7} m^3/s respectively. The values of water and oil absorption rates of the produced brake pads compared well with the standard values of 0.288×10^{-7}–1.314×10^{-7} m^3/s and 0.0×10^{-7}–0.53×10^{-7} m^3/s respectively given by the inertia dynamometer, and compared well with the value of 1.18×10^{-7} m^3/s obtained by the commercial pad.

3.9. Temperature

The variation of temperature with speed is presented on Fig. 12. It was observed that temperature rises linearly with increase in speed as similar findings were reported by Liew and Nirmal (2013). The temperature rise for brake pads produced varied from 102–735 °C and compared well with the value of 527 °C reported by Talib et al.,(2012) and 650 °C obtained by the commercial pad.

3.10. Stopping time

Stopping time is the time taken by the brake pads to bring the vehicle to a halt and normally tends to increase as the speed increases. Fig. 13 presents the variation of stopping time with speed, and indicates that stopping time increased from 5.56 to 27.78 m/s, thus agreeing with the trend reported by Ibhadode and Dagwa (2008). Values of stopping time for the PKFs brake pads varied from 3.1 to 9.1 s; these are better than the value of 4.1 s reported by Ibhadode and Dagwa (2008) and 4.09 for the commercial brake pad at 27.78 m/s.

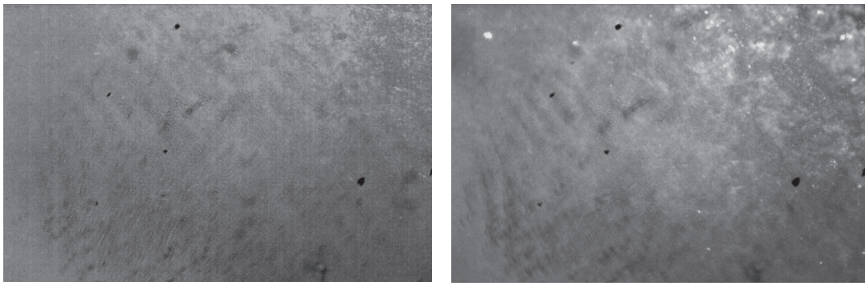

(a) (b)

Figure 16 Surfaces of (a) unworn and (b) worn for sample S_1.

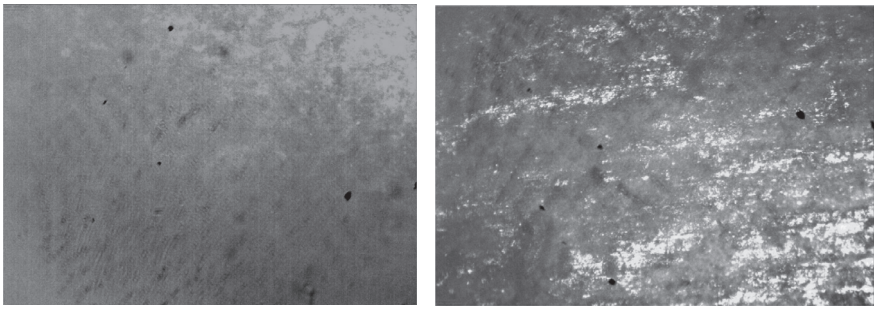

(a) (b)

Figure 17 Surfaces of (a) unworn and (b) worn for sample S_2.

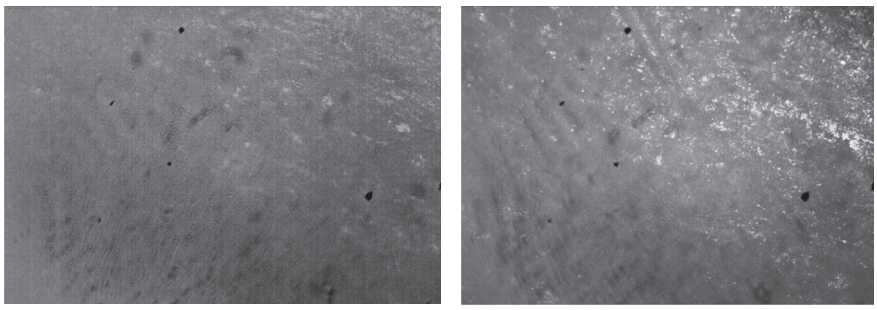

(a) (b)

Figure 18 Surfaces of (a) unworn and (b) worn for sample S_3.

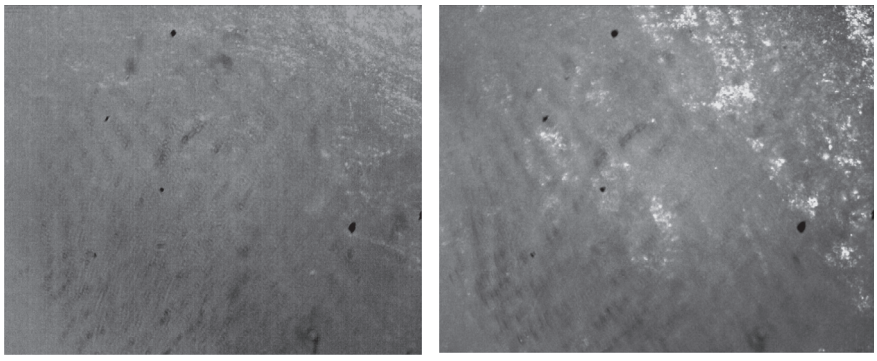

(a) (b)

Figure 19 Surfaces of (a) unworn and (b) worn for sample S_4.

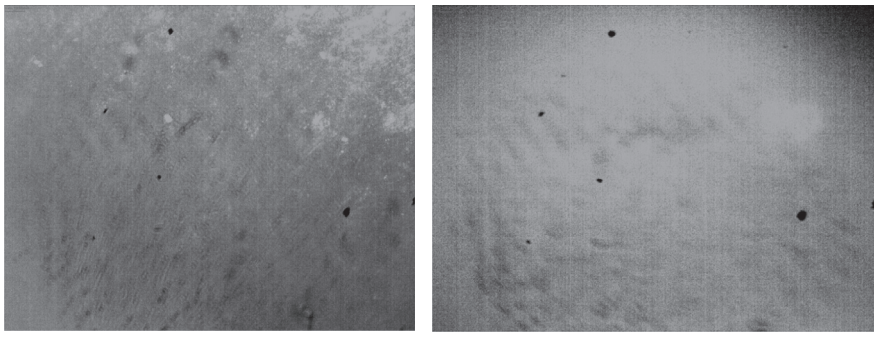

(a) (b)

Figure 20 Surfaces of (a) unworn and (b) worn for sample S_5.

3.11. Specific gravity

As shown in Fig. 14 the specific gravity of the produced brake pads, did not vary with increasing speed. The specific gravity of produced samples varied from 1.7 to 2.1, and values agreed with the values of 1.161–1.89 reported by Efendy et al. (2010), and compared well with the value of 2.06 obtained by the commercial pad.

3.12. Surface roughness

Fig. 15 shows the surface roughness of the produced brake pads along with the commercial pad. It was also observed that surface roughness remained constant with increased speed. The surface roughness of produced samples varied from 2.3 to 3.72 and agreed with the values of 2.04–2.97, reported by WanNik et al. (2012).

3.13. Microstructure examination

The microstructure examinations of unworn and worn surfaces for produced brake pads are shown on Figs. 16–21. It was indicated that the friction materials were made up of different additives. The white region on the surface indicated the fibres from the PKFs, the black spots indicated the graphite, while the dark region indicated the resin and only graphite

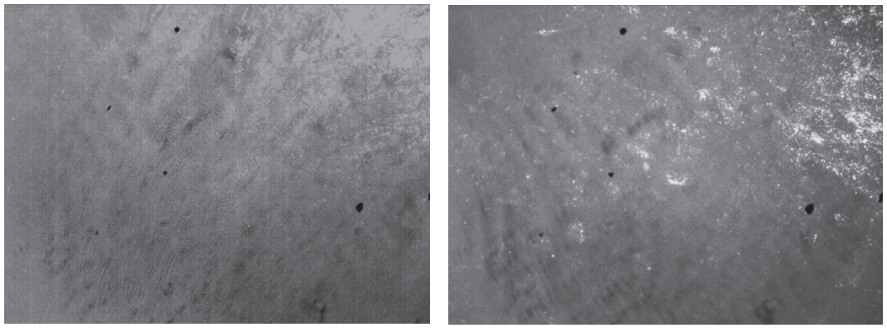

(a) (b)

Figure 21 Surfaces of (a) unworn and (b) worn for sample S_6.

Table 4 Other basic engineering properties.

S/N	Properties	Commercial	S_1	S_2	S_3	S_4	S_5	S_6
1	Mechanical overload	4	2	1	3	3	1	2
2	Thermal deformation	3	1	2	3	3	1	3
3	Fading behaviour	3	1	1	2	3	1	2
4	Shear strength	3	2	1	3	2	1	2
5	Cracking resistance	4	3	1	2	3	1	2
6	Over-heat recovery	3	3	–	3	1	2	2
7	Effect on rotor disc	3	2	1	2	1	1	1
8	Caliper pressure	4	2	2	1	2	1	2
9	Pad grip effect	3	3	3	2	2	2	2
10	Pad dusting effect	2	3	1	2	4	1	1

Rating (s)	Low	Medium	Average	High
Value	1	2	3	4

Evaluation scale.
N.B. – low/medium bad product; average/high good product.

Table 5 Comparison of the result with existing findings.

Properties	Commercial brake pad (asbestos based)	Laboratory formulation (palm kernel shell)	Laboratory formulation (Banana peel)	New laboratory formulation (palm kernel fibres)
Wear rate (mg/m)	3.80	4.4	4.67	3.98
Coefficient of friction	0.316	0.43	0.35	0.33
Porosity (%)	18	22.45		22
Hardness (h)	9.83	–	–	10
Water absorption rate $\times 10^{-7}$(m^3/s)	1.18	–	–	1.84
Oil absorption rate $\times 10^{-7}$ (m^3/s)	0.39	–	–	0.26
Surface roughness	3.03	–	–	3.02
Temperature (°C)	650			650
Specific gravity	2.06	1.65	1.8	2.1
Moisture effect (%)	1.01	–	–	1.02
Noise level (dB)	40	–	–	30
Stopping time (s)	4.09	4.12	–	3.9

black spots were not covered by friction material this confirms the observation reported by Idris et al. (2015). No crack or degradation of the additives was observed on the examined surfaces supporting that the surfaces had high wear resistance.

The surfaces were observed to be characterized by abrasion wear where the asperities were ploughed thereby exposing the white regions (PKFs fibre) on the surfaces, thus increasing the smoothness of the friction materials. This could be appreciated if one compares the surface of sample S_5 on Fig. 20 (b) with the surface of S_1 on Fig. 21(b), where the S_5 showed smoother surface topography which was responsible for high wear rate (9.21 mg/m) compared with the S_1 (3.62 mg/m). It was also observed that the graphite spots on the worn surfaces became more exposed indicating that friction materials have undergone wear compared to the unworn surfaces as shown in Figs. 16–21. The microstructure also revealed wear grooves parallel to disk rotation and this confirms the observation reported by Koya and Fono (2010).

3.14. Other basic engineering properties

Values of other engineering properties (mechanical overload, thermal deformation, fading behaviour, shear strength, cracking resistance, over-heat recovery, effect on rotor, caliper pressure, pad grip effect, and pad dusting effect) evaluated at constant speed of 27.78 m/s (100 km/h) are presented in Table 4. It was observed that most of the properties agreed with the values obtained by commercial brake using an evaluation scale of 1–4 (scale values of 1, 2, 3, and 4 represented low, medium, average and high respectively). Most values were in the range of Average and this is considered an indication of a good product.

4. Conclusions

The evaluation of brake pads developed from palm kernel fibres was determined and the conclusions are summarized as follows:

1. That values of the necessary parameters obtained from PKFs are within (and even better) the standard requirement for commercial brake performance pad.
2. Sample S_2 exhibited the highest coefficient of friction (0.4) but higher wear rate (7.21 mg/m), implying that the friction materials will be efficient but shorter life span.
3. Samples S_6 with composition of 40% epoxy-resin, 10% palm wastes, 6% Al_2O_3, 29% graphite, and 15% calcium carbonate gave better properties than other samples tested as compared to other findings presented on Table 5.
4. Palm kernel fibre (PKFs) can be a suitable replacement to asbestos for brake pad production.

References

Aigbodion, V.S., Akadike, U., Hassan, S.B., Asuke, F., Agunsoye, J.O., 2010. Development of asbestos- free brake pad using bagasse. Tribol. Indus. 32, 12–18.

Chand, N., Hashmi, A.R., Lomash, S., Naik, A., 2004. Development of asbestos free brake pad. J.-MC 85, 13–16.

Efendy, H., Wan Mochamad, W-M., Yusuf, N.B.M., 2010. Development of natural fiber in Non-metallic brake friction material. Seminar Nasional Tahunan Teknik Mesin (SNTTM), 13–15, Ke-9 Palembang.

El-Tayeb, N.S.M., Liew, K.W., 2009. On the dry and wet sliding performance of potentially new frictional brake pad materials for automotive industry. Wear 266, 275–287.

Ibhadode, A.O.A., Dagwa, I.M., 2008. Development of asbestos-free friction lining material from palm kernel shell. J. Braz. Soc. Mech. Sci. Eng. 1 (1), 1–2.

Idris, U.D., Aigbodion, V.S., Abubakar, I.J., Nwoye, C.I., 2015. Eco-friendly asbestos free brake-pad: using banana peels. J. King Saud Univ.-Eng. Sci. 27 (2), 185–192.

Jang, H., Ko, K., Kim, S.J., Basch, R.H., Fash, J.W., 2004. The effect of metal fibres on the friction performance of automotive brake friction materials. Wear 256, 406–414.

Kim, S.S., Hwang, H.J., Ho Jang, M.W., 2011. Friction and vibration of automotive brake pads containing different abrasive particles. Wear 271, 1194–1202.

Koya, O.A., and Fono, T.R (2010). Palm kernel shell in the manufacture of automotive brake pad (accessed at www.rmrdc-technoexpo.com, 7/3/210).

Liew, K.L., Nirmal, U., 2013. Frictional performance evaluation of newly designed brake pads materials. Mater. Des. 48, 25–33.

Lindberg, E., Horlin, N-E., Goransson, P., 2013. An experimental study of interior Vehicle roughness noise from disc brake systems. Appl. Acoust. 74, 396.

Namessan, N.O., Maduako, J.N., Iya, S.A., 2012. Comparative study of the effects of treatment techniques on the thermal, friction and wear properties of kenaf (*Hibiscus cannabinus*) fibre reinforced brake pads. Eur. J. Sci. Res. 76, 660.

Oberst, S., Lai, J.C.S., 2011. Statistical analysis of brake squeal noise. J. Sound Vib. 330, 2978–2994.

Ruzaidi, C.M., Kamarudin, J.B., Shamsul, J.B., Mustafa Al Barkri, A.M., Rafiza, A.R., 2011. Comparative study on thermal, compressive, and wear properties of palm slag brake pad composite with other fillers. Aust. J. Basic Appl. Sci. 5, 79.

Talib, R.J., Mohmad, S.S., Ramlan, K., 2012. Selection of best formulation for semi-metallic brake friction materials development. Powder metallurgy (accessed at www.intechopen.com), 1–30.

WanNik, W.B., Ayob, A.F., Syahrullail, S., Masjuki, H.H., Ahmad, M.F., 2012. The effect of boron friction modifier on the performance of brake pads. Int. J. Mech. Mater. Eng. 7, 31.